



# Pharmaceutical and biomaterial engineering via electrohydrodynamic atomization technologies

Prina Mehta<sup>1</sup>, Rita Haj-Ahmad<sup>1</sup>, Manoochehr Rasekh<sup>1</sup>,  
Muhammad S. Arshad<sup>1</sup>, Ashleigh Smith<sup>2</sup>, Susanna M. van der Merwe<sup>2</sup>,  
Xiang Li<sup>3</sup>, Ming-Wei Chang<sup>4,5</sup> and Zeeshan Ahmad<sup>1</sup>



<sup>1</sup> Leicester School of Pharmacy, De Montfort University, Leicester LE1 9BH, UK

<sup>2</sup> School of Pharmacy and Biomedical Sciences, University of Portsmouth, Portsmouth, PO1 2DT, UK

<sup>3</sup> State Key Laboratory of Silicon Materials, School of Materials Science and Engineering, Zhejiang University, Hangzhou 310027, China

<sup>4</sup> College of Biomedical Engineering and Instrument Science, Zhejiang University, Hangzhou 310027, China

<sup>5</sup> Zhejiang Provincial Key Laboratory of Cardio-Cerebral Vascular Detection Technology and Medicinal Effectiveness Appraisal, Zhejiang University, Hangzhou 310027, China

**Complex micro- and nano-structures enable crucial developments in the healthcare remit (e.g., pharmaceutical and biomaterial sciences). In recent times, several technologies have been developed and explored to address key healthcare challenges (e.g., advanced chemotherapy, biomedical diagnostics and tissue regeneration). Electrohydrodynamic atomization (EHDA) technologies are rapidly emerging as promising candidates to address these issues. The fundamental principle driving EHDA engineering relates to the action of an electric force (field) on flowing conducting medium (formulation) giving rise to a stable Taylor cone. Through careful optimization of process parameters, material properties and selection, nozzle and needle design, and collection substrate method, complex active micro- and nano-structures are engineered. This short review focuses on key selected recent and established advances in the field of pharmaceutical and biomaterial applications.**

## Introduction

Complex micro- and nano-structures are enabling crucial developments in the healthcare remit (e.g., pharmaceutical sciences), which also demonstrates a shift from conventional coarser and simple technologies. Deviation from established concepts and methodologies relating to drug delivery or biomaterial development is testing and initially met with reservation. However, high-value developments that can overcome barriers for existing concepts or methods, and are able to address key global challenges, are recognizable through research impact and utility. For emerging enabling platform technologies, concept development and novel structure engineering outcomes are achievable in tandem, providing numerous opportunities in technological advances. The pharmaceutical and biomaterial industries are well accustomed with

established micro- and nano-engineering platforms such as spray-drying, freeze-drying, super critical fluid synthesis and microfluidics. Over the past two decades, electrohydrodynamic atomization (EHDA) technologies have been explored in great depth evidenced by the exponential growth in related research article publications. Developments within this technology are also embracing timely areas such as biomedical imaging, regenerative medicine, 3D printing and advanced drug delivery as well as providing much needed complexity to the fiber and particle communities. Furthermore, the technologies are attractive because the processes are facile, one-step, versatile and are operational at ambient conditions, and yield complex nano- and micro-structures pertinent to an array of pharmaceutical and biomaterial applications. These also offer significant advantages over existing technologies that are unsuitable for several materials (e.g., owing to elevated process temperatures and shear stresses) [1] that can compromise the

Corresponding author: Ahmad, Z. (zahmad@dmu.ac.uk)

functionality of biomaterials (e.g., proteins) or active pharmaceutical ingredients (APIs) [1–3].

The underlying principle of EHDA processes is based on utilizing an electrical force to atomize liquids; which electrically imposes (electro) a liquid (hydro) jet (dynamic) out of a liquid-filled (infused) nozzle in the form of a jet. Jetting behavior and process parameters predominantly enable particle or fiber synthesis – the simplest form of EHDA engineering. These architectures can then be collected onto an electrically grounded substrate positioned under the tip of the nozzle. The production of a variety of structures can be achieved by varying processing parameters (formulation flow or infusion rate, applied voltage and deposition distance) and physical properties of the liquid (viscosity, density, surface tension and electrical conductivity). Materials for formulation development are often characterized for such properties because these significantly affect jetting stability [4] as well as morphology and phase of engineered structures [5].

EHDA jets are established and characterized by evaluating two parameters: intensity and droplet diameter (both of which are affected by physical liquid properties and the process parameters). EHDA modes are classified into two categories (depending on how the liquid jet breaks up into droplets): (i) dripping mode (occurs when only fragments of liquid exit from the nozzle); and (ii) jetting mode (observed when the formulation liquid breaks up into fine droplets some distance from the nozzle exit) [4] (Fig. 1).

There are two main forms of EHDA processes: electrospraying (ESy; particle production); and electrospinning (ES; fiber production), and they serve as promising enabling technologies for a range of applications [6]. This review focuses on crucial, and the most recent, developments in EHDA technologies and their various applications related to pharmaceutical and biomaterial sciences. Examples of structures generated using EHDA technologies (single and co-axial nozzles, printing, multiple nozzles, nonconcentric nozzles and multiphase generation) are provided. Table 1 summarizes key selected developments in this area. Fig. 2 shows examples of various structures produced using EHDA technologies.

## Single nozzle

The first and simplest EHDA configuration consists of a single nozzle through which formulation (API–polymer solution) is infused and atomized using an electrical force. The API is typically incorporated into a polymer–solvent solution, although numerous excipients can also be added to increase complexity or modify functionality. During the atomization process, which includes rapid solvent evaporation, the API is uniformly dispersed throughout the polymeric matrix, which is also a means to enhance the amorphous form of crystalline drug [7]. The potential of single nozzle systems has been demonstrated using a large selection of active biomaterials (e.g., synthetic bone minerals, proteins and peptides) and the encapsulation of genes and anticancer and other bioactive agents [8].

Insulin (a hormone produced by the pancreas) was one of the first biomolecules to be utilized for the ESy process. Near-mono-dispersed insulin-loaded nanoparticles (NPs) were produced using a single nozzle system (variable flow rates of  $\sim 0.17$ , 0.24 and 0.38  $\mu\text{l}/\text{min}$  and applied voltage of  $\sim 5$  kV) sufficient to yield NPs in the range of 98–117 nm. Gomez *et al.* found that, by decreasing the concentration of insulin in solution or by reducing the flow rate of the ESy system, smaller particles can be generated [9]. More recently, *N*-acetylcysteine (NAC)-loaded poly(lactic-co-glycolic acid) (PLGA) NPs were also synthesized using a single nozzle ESy technique (flow rate  $\sim 0.06$ –0.18 ml/h and applied voltage  $\sim 10$  kV) [10]. NAC is a thiol-containing compound used for the treatment of bronchitis, cystic fibrosis, emphysema and pneumonia with poor oral bioavailability (4–10%). By optimizing process conditions, resulting particles were as small as 122 nm with drug encapsulation efficiency (EE) of  $\sim 54.5\%$ . These were achieved by reducing the flow rate and matrix polymer (PLGA) concentration. Particles exhibited a biphasic release profile – an initial burst release followed by a more sustained release [10].

Other proteins have also been encapsulated to prepare biomaterial scaffolds (fibrous structures) using the single nozzle ES process to facilitate neo-tissue development. Electrospun fibrous

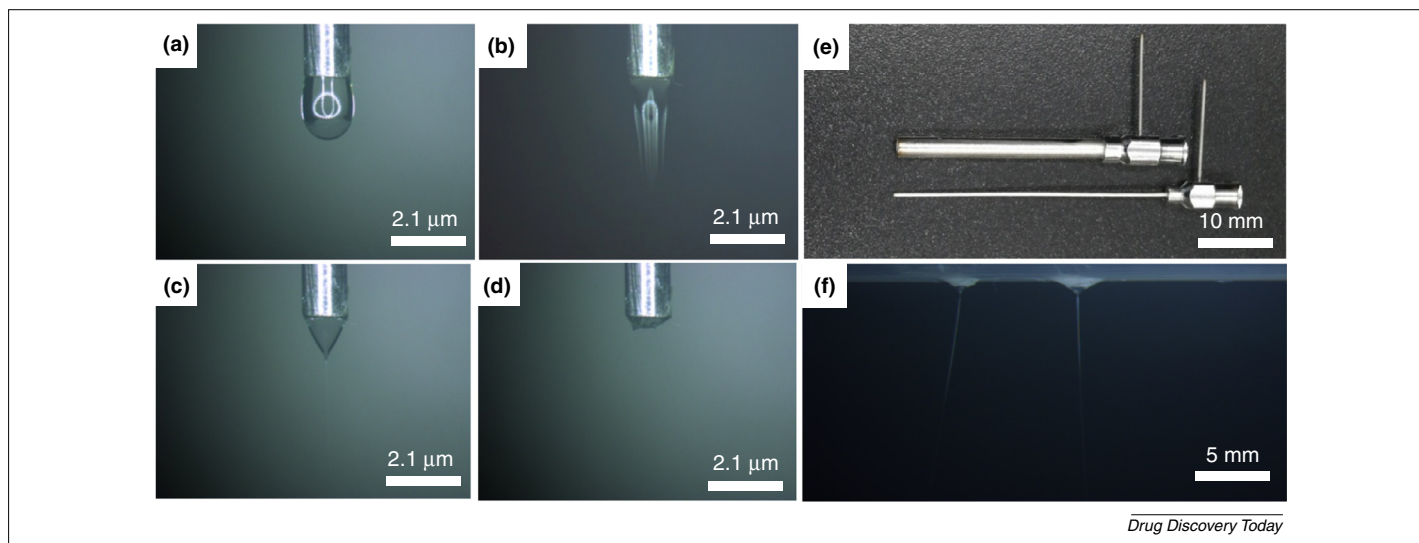


**FIGURE 1**

EHDA jetting examples from a single nozzle system showing: (a) Formulation flow with no applied voltage – dripping; (b) unstable jetting; (c) stable jetting – Taylor cone; (d) multiple-jets from a single nozzle. (e) The coaxial nozzle system used for jetting with two co-flows (inner and outer nozzles). (f) Stable jetting from two pores (nozzle-less approach). Formulation used for jetting examples polycaprolactone (5% (w/v)) and dichloromethane.

TABLE 1

## A summary of key selected developments in various EHDA technologies.

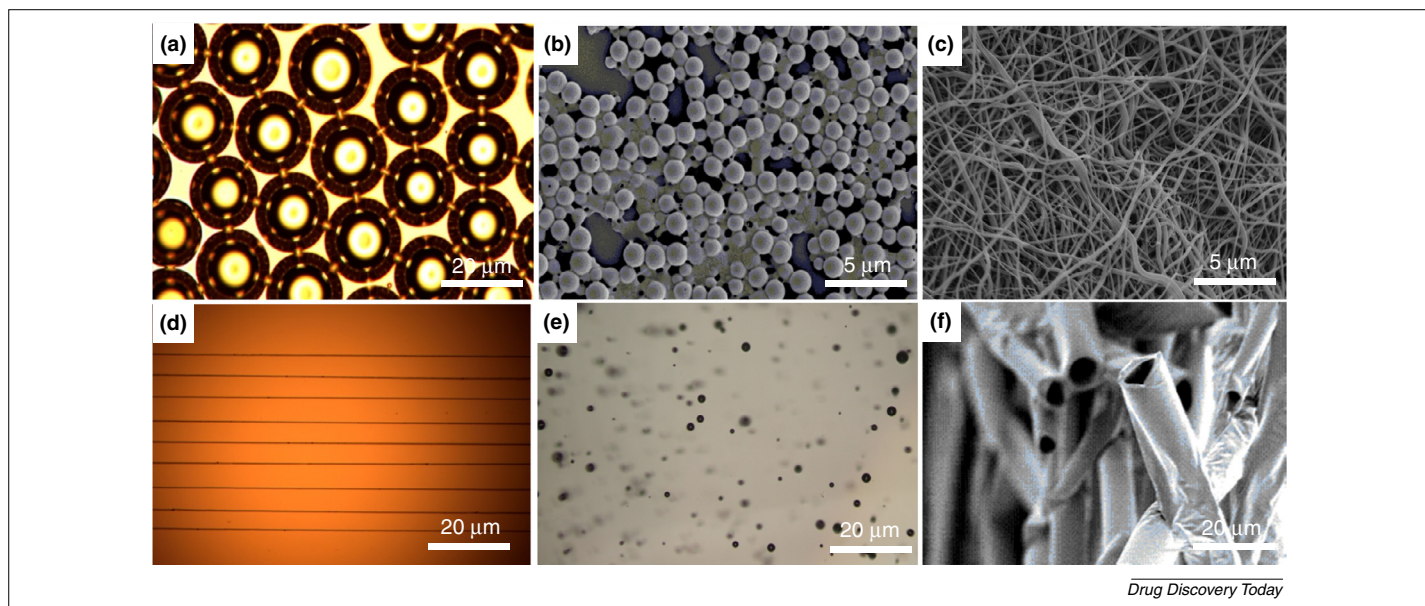
EHDA method	Nozzle/ needle geometry	Nozzle size (mm)	Active/ encapsulated material	Application	Particle/fiber diameter ( $\mu\text{m}$ )	Materials for matrix or encapsulant	Comments	Refs
Electrospraying	Single	Not specified	N-acetylcysteine	Amino acid delivery	0.122	PLGA	Box–Behnken design was used to find optimum parameter settings. Smallest size and smallest polydispersity: flow rate (0.06 ml/h), polymer concentration (0.5% (w/w)), collecting distance (9.28 cm) and encapsulation efficiency of 54.5%	[10]
	Single	0.55	Cisplatin	Anticancer drug delivery	0.059	Silk fibroin	Release of cisplatin was sustained for more than 15 days. Sufficient apoptosis of A549 lung cancer cells was observed with less toxicity to L929 mouse fibroblast cells	[20]
	Coaxial	Outer nozzle: 1.9 Inner nozzle: 0.9	Angiotensin II	Peptide hormone delivery	0.1–0.3	Tristearin	Clear core–shell structure was observed with triphasic release kinetics; initial burst followed by sustained and finally conventional diffusion	[25]
	Coaxial	Outer nozzle: ID: 1.0 Inner nozzle: OD: 0.5 ID: 0.3	Metronidazole	Antibiotic	0.06–0.389 (depends on PMMA percentage)	PMMA, Eudragit®/RS	The porous hydrophilic core/ hydrophobic shell NPs exhibited slow release of drug. Capsules maintained their size for over 8 h as a result of bioinert nature of PMMA. Cellular internalization analysis confirmed safety of the prepared NPs	[29]
	Co-axial	Outermost: OD: 4 ID: 3.2 Second outermost: OD: 2.6 ID: 2.0 Second innermost: OD: 1.5 ID: 1.0 Innermost: OD: 0.5 ID: 0.2 ID: 0.6	Hermatoxylin dye, pinacyanol chloride, pyronin, Evans blue	Multiple dye loading and release	$0.620 \pm 0.150$	PEG, PLGA, PCL, PMSQ	A four-nozzle device was utilized to produce four layered particles and fibers. TEM demonstrated four distinct layers whereas <i>in vitro</i> release studies indicated combination of release mechanisms, dissolution and diffusion	[24]
	Single		Red blood cells	Imaging using MRI and fluorescence	0.0044–0.005	EHEC, HPC, CEC, dextran, PEG, PMMA	The blood-cell-shaped polymeric particles were able to pass through channels that were smaller than the particles themselves; enabling improved circulation in blood. Encapsulation of dye indicates multifunctional capabilities of these biodegradable particles	[39]
Electrospinning	Single	Not specified	siRNA	Gene therapy	0.3–0.4	PCL, PEG	Fibers released siRNA for a minimum of 28 days and exhibited 61–81% silencing efficiency.	[16]
	Single	OD: 0.64 ID: 0.33	Piroxicam	Anti- inflammatory action	11.4	No matrix	A new polymorph resulted that was verified by using various spectroscopic techniques. FTIR showed new chemical bonds as well as new functional groups present in the sprayed piroxicam	[21]
	Coaxial	Outer nozzle: OD: 0.9 Inner nozzle: OD: 0.63 ID: 0.33	Doxorubicin	Anticancer drug delivery	0.284 (mean diameter of doxorubicin- loaded micelles-loaded coaxial NF)	Gelatin, PVA	Biodegradable polymeric NFs embedded with micelles provided another barrier for drug diffusion, hence providing sustained release of doxorubicin	[32]
	Coaxial	Outer nozzle: OD: 1.15 ID: 0.99 Inner nozzle: OD: 0.6 ID: 0.3	Doxorubicin	Anticancer drug delivery	0.235	PVA, chitosan	Biocompatible NFs had less cytotoxicity compared with free doxorubicin; whereas <i>in vitro</i> release experiments showed drug release rate was controllable. The resulting fibers also promoted attachment, proliferation and spreading of human ovarian cancer cells (SKOV3)	[31]
	Coaxial	Outer nozzle: OD: 1.5 ID: 1 Inner nozzle: OD: 0.4 ID: 0.2	Ketoconazole	Antifungal	Optimal $8.7 \pm 7.2$	PCL	Hollow PCL fibers loaded with magnetic Fe <sub>3</sub> O <sub>4</sub> particles and ketoconazole. Release mainly diffusive but expedited with external trigger using an auxiliary magnetic field	[38]

TABLE 1 (Continued)

EHDA method	Nozzle/ needle geometry	Nozzle size (mm)	Active/ encapsulated material	Application	Particle/fiber diameter ( $\mu\text{m}$ )	Materials for matrix or encapsulant	Comments	Refs
<b>Bubbling</b>	Coaxial	Outer nozzle: OD: 1.1 ID: 0.685 Inner nozzle: OD: 0.3 ID: 0.15	Air	Imaging and drug delivery potential	Different sizes but all below 10	Phospholipid	High yield of MBs ( $10^9$ bubbles/min) stable over 2.5 h at physiological temperature ( $37^\circ\text{C}$ ), MB size decreased rapidly to $1.3 \pm 0.4 \mu\text{m}$ within 50 min	[50]
	Coaxial	Outer nozzle: 2.2 Inner nozzle: 1.9	Air, BSA	Biological scaffolds	240–1000	Silk fibroin	Silk fibroin was used to produce MBs that exhibited unique morphology compared with aqueous silk fibroin bubbles. The resulting hollow spherical structures could also serve as porous niches with potential applications in tissue engineering and bio-coatings	[52]
	Coaxial	Outer nozzle: 2.2 Inner nozzle: 1.9	Air, BSA	Biological scaffolds, sensors and drug delivery potential	40–800	BSA, distilled water- glutaraldehyde, glycerol and glycerol- Tween® 80	Increasing the flow rate of BSA solution reduced the polydispersity of MBs and stability test showed bubble size and size distribution stability was enhanced over time. However, MB stiffness increased from 8 N/m to 20 N/m upon increasing BSA concentration in the solution from 5 wt% to 15 wt%	[51]
<b>Printing</b>	Single	OD: 1.175 ID: 0.75	Nano- hydroxyapatite	Biomedical engineering	<5	PCL	Direct writing of nano-hydroxyapatite can be advantageous in biomedical artificial tissue scaffolds. The pores on the resulting tracks can yield various degradation rates as well as diffusion of various molecules from the polymeric matrix	[58]
	Single	ID: 0.5	Tetracycline hydrochloride	Antibacterial	0.7–5.0	PVP PEO PVP–PEO	Antibiotic drug was encapsulated within various polymeric compositions with the ability to control release. Relatively high encapsulation achieved. Facile control on patterning	[59]
	Single	OD: 0.320 ID: 0.05	Silver	Antibacterial potential	0.7	Silver NP ink	Increased resolution in EHD printing by utilizing a hypodermic needle	[54]
	Single	ID: 0.33	Copper oxide	Antibacterial	50	PU	Antibacterial activity (MRSA) using polyurethane-copper oxide film compositions (up to 10 w/w%) shown	[60]
<b>Other technology</b>	Multi-needle electrospinning	OD: 0.6 ID: 0.55	N/A	N/A	Down to 0.2	PEO	Fiber diameter greatly reduced as the number of needles used increased (1, 7, 37 needles). Hexagonal configuration of needles yielded finer fibers owing to more-uniform electric field at needle tips. The more needles used the larger collection distance was required	[41]
	Triaxial electrospinning	Core: OD: 0.55 ID: 0.3 Intermediate: OD: 1.25 ID: 0.85 Sheath: OD: 2.11 ID: 1.6	Keyacid blue, keyacid uranine	Probe (drug or active delivery)		PCL, PVP	Triaxial configuration of needles yielded trilayered fibers that exhibited slower release of probes; providing initial burst release from hygroscopic PCL shell layer and subsequent sustained release from fiber core. The intermediate layer provided an extra barrier to drug diffusion and hence contributed to the sustained release of probes	[43]
	Needle-less electrospinning	N/A	N/A	N/A	0.2–0.8	PEO	Polymeric solution was directed onto a metal roller spinneret; this method proved to be 24–45-times more productive than single needle electrospinning	[44]
	Aligned needles (nonconcentric)	Not specified	PTDPV-dye ADS 306PT-dye	Probe (drug or active delivery). Targeted delivery	$0.423 \pm 0.291$	PLGA, CTAB, PMMA, modified PLGA and PMMA	Janus particles formed through 'co-jetting'. Particles persisted <i>in vivo</i> (murine) for over 24 h but also demonstrated specific targeted capabilities	[48]

**Abbreviations:** OD, outer diameter; ID, inner diameter; ES, electrospinning; ESy, electrospaying; PCL, polycaprolactone; NPs, nanoparticles; NFs, nanofibers; PLGA, poly(lactic-co-glycolic acid); PMMA, poly(methyl methacrylate); HCPT, hydroxycamptothecin; PVA, poly(vinyl alcohol); BSA, bovine serum albumin; MBs, microbubbles; PVP, polyvinyl pyrrolidone; MRSA, methicillin-resistant *Staphylococcus aureus*; CTAB, cetyl trimethylammonium bromide; PEO, polyethylene oxide; PU, polyurethane; PEG, polyethylene glycol.



**FIGURE 2**

Examples of structures generated using EHDA technologies showing (a) core-shell PCL microcapsules via coaxial electrospinning, (b) solid PLGA matrix-type microparticles via single nozzle electrospinning, (c) PVP nanofibers via single-nozzle electrospinning, (d) BSA microbubbles via microbubbling, (e) PVP patterns via printing and (f) PMSQ microtube bundles via coaxial electrospinning. Abbreviations: PVP, polyvinylpyrrolidone; PLGA, poly(lactic-co-glycolic acid); PCL, polycaprolactone; PMSQ, polymethylsilsequioxane; BSA, bovine serum albumin.

PLGA scaffolds incorporating protein [either bovine serum albumin (BSA) or myoglobin] were engineered with different hydrophilicities. Scaffolds ( $468 \pm 139$  nm) exhibited appreciable (80%) protein EE and also displayed potential for dual protein delivery [11]. Luciferase (an oxidative enzyme) has also been loaded into polyvinyl alcohol (PVA) fibers using a single nozzle system. Luciferase retained its enzymatic activity after ES fabrication and continuous release of the enzyme from PVA nanofiber matrix was shown [12].

DNA-based pharmaceuticals for the treatment of various diseases (such as acute respiratory distress syndrome, asthma, cystic fibrosis and cancer) have interestingly increased in number. Zeles-Hahn *et al.* demonstrated the potential to administer DNA-based therapeutics in the form of aerosols to the pulmonary system. Naked and complexed plasmid DNA-polyethyleneimine aerosols were fabricated using ESy (flow rate of 0.2 ml/min and applied voltage range  $\sim 0$ –6 kV) using a single nozzle system, with no indication of structural alteration or loss of DNA integrity and minimum cell toxicity [13].

One of the earliest studies that used ES for DNA-based applications transpired in the late 1990s, where calf-thymus Na-DNA fibers (50 and 80 nm) were produced [14]. More recently, focus has been directed toward the potential of encapsulating and delivering siRNA because of extracellular limitations (degradation and specific cell targeting) and intracellular limitations (endosomal escape and mRNA targeting) [15]. Whereas therapeutic applications of siRNA are often in the form of NPs, for emerging applications such as tissue regeneration electrospun fibers offer a cost-effective and simple alternative to achieve encapsulation and sustained activity. For example, electrospun siRNA-loaded polycaprolactone (PCL) fibers (300–400 nm) demonstrated siRNA release for 28 days at physiological conditions [16].

The administration of anticancer drugs to a specific site of action (to provide therapeutic effect) is often met with numerous challenges. Physical properties (such as drug solubility and poor drug pharmacodynamics) can prevent therapeutic drug concentrations from reaching the site of action, resulting in frequent administration. Cyclophosphamide (INN) is an anticancer drug that is used for the treatment of various cancer types such as retinoblastoma, neuroblastoma and breast cancer. It functions by disrupting DNA replication or can be combined with DNA (combined therapy) to inhibit tumor growth [17].

Gulfam *et al.* synthesized a potent tool for the delivery of INN with controlled-release properties. Gliadin NPs and gliadin-gelatin composite NPs loaded with INN were produced using the single nozzle ESy technique. The loading efficiency of NPs was  $72.02 \pm 5.6\%$ . In comparison with gliadin-gelatin composite NPs, gliadin NPs demonstrated a gradual drug release for 48 h whereas gliadin-gelatin composite NPs showed a rapid drug release. Moreover, breast cancer cells cultured with 7% INN-loaded gliadin NPs led to apoptosis after 24 h [18].

Silk-based NPs have been successfully developed to aid the delivery of proteins, small molecules and APIs including anticancer drugs [19]. Silk fibroin, a naturally occurring protein, has been used as a novel nanocarrier for anticancer drugs, engineered using the EHDA process. To maintain the therapeutic activity of *cis*-dichlorodiamminoplatinium (cisplatin), the active was loaded into silk fibroin NPs by single nozzle ESy. NPs ( $\sim 59$  nm in diameter) demonstrated slow and sustained release of cisplatin for more than 15 days whereas *in vitro* anticancer studies exhibited apoptosis of A549 lung cancer cells but showed weaker interactions with normal healthy cells [20].

The EHDA process has also been used to vary polymorphic forms of drugs. For example, piroxicam (polymorphic form I)

was dissolved in chloroform and then electrosprayed (flow rate  $\sim 2.5$ – $3.0$  ml/h and applied voltage range  $\sim 2.7$ – $4.1$  kV) using a single nozzle system. The resulting polymorph displayed an unknown crystal structure when examined using X-ray diffraction (XRD), Fourier transform infrared (FTIR) and Raman spectroscopy. Comparisons between FTIR spectra and XRD showed evident changes in structure, new functional groups and chemical bonds. The particles (diameter  $\sim 11.4$   $\mu\text{m}$ ) were spherical in shape and showed no signs of degradation over 127 days of storage [21].

In recent times, pharmaceutical and biomaterial applications have diversified and evolved for more-complex forms of dosage development and delivery (e.g., multimodal drug action for par-enteral delivery) [1,22]. For example, rapidly dissolving polyvinylpyrrolidone (PVP) was used to develop double-sided coatings and multifunctional contact lenses [1]. PVP NPs less than 100 nm in size and PVP nanofibers (NFs) less than 200 nm in diameter were utilized as active ocular lens coatings, demonstrating model probe release and antibacterial properties.

### Coaxial arrangement

Coaxial EHDA (co-EHDA) is the term used to describe the use of two conductive nozzles in conjunction in a coaxial arrangement. This configuration can be utilized for one-step encapsulation of APIs and therapeutic agents within a polymeric shell or matrix. The materials used within this system are ideally immiscible; therefore, coaxially aligned nozzles produce particles with a defined shell (polymer) and a defined core (therapeutic agent). Loscertales *et al.* were the first to propose the use of coaxial nozzles. Using a coaxial set-up, capsules (inner nozzle: water; outer nozzle: olive oil) ranging in size between 150 nm and 10  $\mu\text{m}$  were produced [23]. In the coaxial arrangement, the medium with greater electrical conductivity is the driving force and, therefore, materials possessing very low electrical conductivities can be engineered using co-flow under an electrical field. Although the vast majority of co-EHDA research has focused on two concentric nozzles, the potential to use three or more [3,24] nozzles has also been demonstrated for compartmentalization within particles for biomedical applications, including the use of multiple model materials and phases.

Co-EHDA has been used to produce complex structures, encapsulating biomacromolecules such as peptides and proteins without denaturation and degradation. For instance, angiotensin II was successfully encapsulated into tristearin, yielding clear core-shell NPs (diameter  $\sim 100$ – $300$  nm) with EE of  $\sim 92 \pm 1.8\%$ . An *in vitro* triphasic release profile was indicated [25]. Model protein BSA has been encapsulated within a biodegradable PLGA shell yielding particles with diameters between 3 and 5.5  $\mu\text{m}$ . BSA EE was 15.7% and 25.1% higher than emulsion E<sub>Sy</sub> particles for high and low molecular PLGA, respectively; indicating material properties (i.e., molecular weight) and processing variables can have a significant effect on encapsulation of actives during the E<sub>Sy</sub> process [26].

Laelorspoen *et al.* developed zein microparticles (MPs) consisting of an alginate and *Lactobacillus acidophilus* core and acidified zein (shell matrix) to assess the ability to produce EHDA engineered vehicles for microorganism delivery. Here, core-shell structures provided sufficient protection from harsh physiological conditions. The capsules (size range  $\sim 543 \pm 88$  to  $259 \pm 62$   $\mu\text{m}$

depending on the applied voltage) improved the survival of the probiotic bacterium fivefold in stimulated gastric fluid [27].

Ongoing developments (and optimization) in EHDA processes and careful selection of formulation materials has made the concept of controlled production of miniaturized capsules a reality [28–30]. Alginate micro- and nano-capsules (range  $\sim 80$  nm to 900  $\mu\text{m}$ ) were generated for the encapsulation of essential oils [28]. Particles 60 nm in size loaded with metronidazole were also synthesized using the co-EHDA process. The antimicrobial, anti-protozoal agent was loaded into Eudragit<sup>®</sup> RS/poly(methyl methacrylate) (PMMA) core-shell particles at an applied voltage of  $\sim 15$  kV. The amphiphilic (hydrophobic shell, hydrophilic core) metronidazole nanocapsules exhibited EE of  $100.2 \pm 0.92\%$  by using 2% PMMA. Porous amphiphilic NPs have potential to be used in various clinical and pharmaceutical applications encapsulating a variety of therapeutic agents, especially where two separate phases are needed [29]. Where this is not essential, multiple actives can be encapsulated into a composite system. For example, dual drug release has been demonstrated using PVP-PLGA and PCL-PLGA composites. NPs (with EE of  $>85\%$ ) of hydrophilic rhodamine B and hydrophobic naproxen were synthesized [30].

Although matrix-type encapsulation of anticancer drugs is achievable using single nozzle systems, co-EHDA provides more-complex structures (e.g., layering) for encapsulation. For example the generation of core-shell fibers encapsulating anticancer drugs has exhibited controlled and sustained drug release and has demonstrated prohibition of cancer cell attachment and proliferation [31,32]. Yang *et al.* developed an implantable device that exploited the amphiphilic nature of micelles and broad application of polymeric NFs. Hydrophobic doxorubicin was entrapped into micelles which formed the core of gelatin fibers along with PVA. The development of this biodegradable device reduced the drug dose required to be administered as well frequent administration, while providing sufficient therapeutic effect against cancerous tissue [32].

The co-EHDA process can also be used for the advanced delivery of anti-inflammatories. Ibuprofen (IBU) delivery systems have been developed as triple-component nanocomposites [33] and NFs [34]. Zein (a prolamine protein) was used to distribute ibuprofen (the core) evenly into *N,N*-dimethylformamide fibers [34]. Qian *et al.* developed triple-component nanocomposites [IBU-PVA-polyacrylonitrile (PAN)] possessing mean diameters of  $620 \pm 120$  nm with 10.5% PVP content. Compared with double-component nanocomposites (IBU-PAN), the triple-component structures significantly improved *in vitro* IBU release kinetics, preventing IBU immobilization within insoluble PAN molecules [33].

BSA has been frequently used as a model protein to demonstrate the delivery of proteins using co-EHDA [11,35]. Electrospun fibrous scaffolds have been developed in which two proteins have been incorporated to provide structural support as well as to stimulate tissue regeneration. BSA and myoglobin were separately integrated into PLGA-Pluronic<sup>®</sup> F-127 fibrous scaffolds ( $423 \pm 209$  nm) with a loading efficiency of  $\sim 80\%$ ; proving to be a useful dual protein delivery system for tissue engineering applications [11]. More recently, electrospun poly(L-lactic acid) (PLLA)-gum-tragacanth NFs were developed that exhibited promising capabilities as grafts for nerve tissue regeneration, high cell

differentiation as well as higher proliferation. Addition of gum tragacanth increased hydrophilicity of PLLA scaffolds as well as NF diameter ( $226 \pm 73$  nm) as a result of increased electrical conductivity [36].

Many co-axial studies have focused on the generation of a core-shell, which will impact the release or encapsulation of active (e.g., drug). Therefore, the ability to control shell thickness is crucial in developing tailored therapies. Gao *et al.* have prepared PCL-shell MPs, encapsulating hydrophobic Sudan Red (a model hydrophobic active in a silicone oil solution) [37]. The resultant structures (30–70  $\mu\text{m}$ ) had controllable shell-thickness:radius (T:R) ratios and exhibited initial burst release followed by sustained release, tunable by the T:R ratio. The ability to encapsulate actives within a polymeric shell using a coaxial set up is further advantageous for the delivery of oil-based materials or hydrophobic actives, which cannot be achieved using such materials alone.

Shell material variation in EHDA engineered structures enables the development of stimuli-responsive materials (e.g., through external triggers), which are gaining interest in biomedical engineering. However, encapsulation of non-polymeric functional materials has advanced the field further. For example, Wang *et al.* have prepared hollow PCL fibers encapsulated with magnetic  $\text{Fe}_3\text{O}_4$  and antifungal drug in the core-shell matrix [38]. The application of an external auxiliary magnetic field enhanced drug release, with the potential to control drug release *in situ* as an on-demand process. Furthermore, the embedded magnetic particles are also able to provide imaging potential. Using similar magnetic NPs and fluorescent dye for encapsulation, red-blood-cell-like polymer particles were engineered using a single nozzle ESy process. Here, dual imaging modality was shown for dark [magnetic resonance imaging (MRI)] and fluorescing phases [39].

### Complex multiple nozzle systems

Advances in EHDA methods have extended toward the development of multi-nozzle or emitter devices that are able to produce particles and fibers in greater capacity and/or complexity [40]. The use of several nozzles and syringes within the process allows the fabrication of fibrous mats such as tissues from multi-jets (Fig. 1f). This system is more complex than single nozzle or coaxial (two nozzles) processes owing to the repulsion that is induced between similarly charged jets. Multi-nozzle systems require a well thought out configuration of nozzles to optimize ES and ESy productivity. Nozzles can be configured in various geometries for example circular, triangular or hexagonal as demonstrated by Yang *et al.* [41]. Preliminary simulation studies showed that using outer nozzles in a hexagonal format assisted in the creation of a uniform electric field near the tips of nozzles, yielding finer polyethylene oxide (PEO) fibers (down to 200 nm) [41].

Biodegradable multilayered NFs have been fabricated by Liu *et al.* using a triaxial (three nozzle) ES set-up [42]. PCL (intermediate layer) and gelatine (sheath and core) were electrospun and fibers of 25  $\mu\text{m}$  were generated, showing the ability to manufacture multilayered NFs with various applications in biotechnology [42]. Triaxial NFs were utilized to demonstrate release profile control of separately encapsulated model drugs (color dyes: keyacid blue and keyacid uranine). PCL and PVP were used to produce triaxial NFs demonstrating sustained release of probes, which was 24-times slower than the release of the same drugs from fibers

produced using coaxial ES. Moreover, triaxial NFs are effective in providing short-term treatment by rapid release of drug entrapped in the outer sheath layer and also for long-term treatment, via sustained release, of drug entrapped in the fiber core [43].

A novel approach for ES was developed by Yarin and Zussman, utilizing a nozzle-less system with a magnetic suspension and magnetic field to force the suspension through a polymer solution, resulting in NFs that ranged from 200 to 800 nm in size. Perturbation of the polymer layer by the ferromagnetic suspension led to a 12-fold enhancement of the production rate of the ES process [44]. Bocanegra *et al.* also developed a nozzle-less system that used orifices rather than nozzle capillaries to achieve a steady jet for atomization of liquids [45]. The system (consisting of up to 37 pores) was found to increase the stability and reliability of the EHDA process. The orifices were arranged in a planar hexagonal pattern with each delivering a cone-jet in the multispray system, which behaved independently from adjacent jets. The multipore system was electrically stable, regardless of pore number or orifice diameter. Jet-bending (from electrostatic interactions with neighboring jets) has been demonstrated using a flute-like horizontal device for the high-throughput production of PCL MPs [46]. The novel device utilized a multipore design instead of nozzle capillaries where modifying pore configuration and processing parameters (applied voltage) yielded uniform MPs. The spatial location of these multiple pores was found to have adverse effects on the stability of the jets; electrostatic forces between adjacent jets caused the jets to bend, generating particles with irregular morphologies. By manipulating the spatial locations, these inconsistencies in morphology can be overcome.

Another recent development has moved away from concentric nozzles and focused more on aligned or converging nozzles (also termed co-jetting). Here, atomized materials do not encapsulate one another but rather form composites as segmented compartments. These have been useful for the preparation of several Janus particle systems, which are able to combine functional properties through precursor spraying (for further processing) [47] as well as altering the shape and segment loading volume, which has great potential in targeted drug delivery [48].

Microbubbles (MBs; hollow MPs filled with air) have been developed and utilized in a vast array of applications in the pharmaceutical industry (e.g., ultrasound imaging and biomedical engineering) [49] and their engineering using EHDA provides potential to modify their properties (e.g., drug loading and coating layer type and number) [3] *in situ* during synthesis. Farook *et al.* utilized a coaxial set-up for the production of MB suspensions with MBs possessing biocompatible phospholipid coatings. These MBs were produced at high yield rates ( $\sim 10^9$  bubbles/min) and were found to decrease in size at physiological temperature. The size and shape alleviated and maintained shape at 1–2  $\mu\text{m}$  after 20 min, showing an increase in temperature led to an increase in the diffusion of air through the phospholipid shell [50].

Coaxial configuration of EHDA has also been used to develop protein (BSA) MBs and porous films [51,52] suggesting a novel tool for protein and peptide applications. A combination of high yield and uniform production with easily amendable size modifications show the potential for multiple biomedical applications including tissue engineering. For example, Ekemen *et al.* developed silk fibroin bubbles (240–1000  $\mu\text{m}$ ) with hollow spherical structures



that are able to aid as a pore generator upon dehydration – advantageous in bio-coatings and tissue engineering [52]. Near mono-dispersed BSA-loaded MBs ranging from 40 to 800  $\mu\text{m}$  have been produced that exhibited negligible changes in size over time which could be due to unfolding of BSA within the bubbles or the solvent evaporation rate [53]. These stabilized MBs can be utilized in vital clinical applications such as protein delivery and tissue engineering.

### Electrohydrodynamic jet printing and patterning

Electrohydrodynamic jet (E-Jet) printing is a manufacturing process that can ‘print’ or ‘write’ patterns on various surfaces on micro- and nano-scales [54]. E-Jet printing utilizes an electrical field to drive jet printing through conductive nozzles, allowing the printing process to be controlled by altering the voltage potential. Ions available in the ejected solution are attracted toward a substrate with the aid of the electrical field. This causes the cone jet to deform leading to instability, releasing droplets at the cone apex. There are currently two recognized modes of E-Jet printing: on demand and continuous. Demand mode revolves around the concept of controlling the jet production and emission only occurs when needed at a pulsed applied voltage, resulting in high deposition accuracy. Continuous jet printing utilizes a pulsed voltage, which can subsequently cause destabilization of the cone jet. E-Jet devices use significantly larger capillary nozzles (compared with conventional systems) that can help reduce any capillary blockage leading to easier processing of solutions, especially suspensions or viscous liquids [55].

A range of biomaterials have been fabricated using E-Jet printing. Hydroxyapatite (HA) NPs were suspended in an ethanol-based suspension and subjected to an electric field. The droplets were deposited according to a programmed topography, yielding patterned tracks as small as 50  $\mu\text{m}$  in width. The utilization of HA-NPs has also extended to the regulation of human osteoblast cell attachment and orientation and also has potential in osteoconduction of implants [56].

The capabilities of this technology have also extended to forming or producing architectures for tissue and biomedical

engineering. Nanocomposite biopolymer (polyurethane system containing silicon components for enhanced surface properties) scaffolds for potential organ development were generated. A 3D EHDA print-patterning device yielded threads less than 50  $\mu\text{m}$  according to a predetermined pattern [57], whereas direct printing of PCL with nano-HA nanocomposites deposited smaller (less than 5  $\mu\text{m}$ ), pre-determined structures; and this could be very advantageous in biomedical topographical engineering [58]. More-recent developments have seen EHDA printing of drug (antibiotic tetracycline hydrochloride) loaded PVP composite fibers demonstrating the ability to develop personalized dosage forms without the use of numerous excipients and formulation steps [59]. There is also potential to utilize functional materials that have deposited using EHDA printing but not been explored in great depth for their biological properties (e.g., as antibacterial coatings) [60]. For example, silver NP ink was used as a jetting solution via slanted hypodermic needles. The utilization of slanted nozzles in place of flat orifices increased the resolution in EHD printing with the narrowest line being printed possessing a width of 0.7  $\mu\text{m}$  [61]. Silver nanowires have also been used for E-Jet printing. Here, the mechanical stretching of the jet solution and enhanced electrostatic forces resulted in highly aligned wires on a nanoscale [62].

### Concluding remarks

From the atomization of simple solution droplets to 3D printing, developments in EHDA technologies can uniquely facilitate developments in numerous pharmaceutical and biomaterial remits. Furthermore, recent developments have shown significant scale-up potential (kg/h production rates), which adds to existing advantageous properties of these high value technologies (e.g., controlled deposition, ambient condition operation, complex structure generation and digital engineering) over existing conventional methods.

### Acknowledgments

The authors would like to acknowledge in part De Montfort University Funding, The EPSRC and The Royal Society for their support.

### References

- Mehta, P. *et al.* (2015) New platforms for multi-functional ocular lenses: engineering double-sided functionalized nano-coatings. *J. Drug Target* 23, 305–310
- Xia, Y. and Pack, D.W. (2015) Uniform biodegradable microparticle systems for controlled release. *Chem. Eng. Sci.* 125, 129–143
- Ahmad, Z. *et al.* (2008) Generation of multilayered structures for biomedical applications using a novel tri-needle coaxial device and electrohydrodynamic flow. *J. R. Soc. Interface* 5, 1255–1261
- Jaworek, A. and Krupa, A. (1999) Classification of the modes of EHD spraying. *J. Aerosol Sci.* 30, 873–893
- Xie, J. *et al.* (2008) Encapsulation of protein drugs in biodegradable microparticles by co-axial electrospray. *J. Colloid Interface Sci.* 317, 469–476
- Bohr, A. *et al.* (2014) Application of spray-drying and electrospraying/electrospinning for poorly water-soluble drugs: a particle engineering approach. *Curr. Pharm. Des.* 20, 325–348
- Jafari-Nodoushan, M. *et al.* (2015) Size and morphology controlling of PLGA microparticles produced by electro hydrodynamic atomization. *Polym. Adv. Technol.* 26, 502–513
- Davoodi, P. *et al.* (2014) Coaxial electrohydrodynamic atomization: microparticles for drug delivery applications. *J. Control. Release* 205, 70–82
- Gomez, A. *et al.* (1998) Production of protein nanoparticles by electrospray drying. *J. Aerosol Sci.* 29, 561–574
- Zarchi, A.A.K. *et al.* (2015) Development and optimisation of N-acetylcysteine-loaded poly(lactic-co-glycolic acid) nanoparticles by electrospray. *Int. J. Biol. Macromolec.* 72, 764–770
- Xu, W. *et al.* (2013) Controllable dual protein delivery through electrospun fibrous scaffolds with different hydrophilicities. *Biomed. Mater.* 8, 014104
- Zeng, J. *et al.* (2005) Poly(vinyl alcohol) nanofibers by electrospinning as a protein delivery system and the retardation of enzyme release by additional polymer coatings. *Biomacromolecules* 6, 1484–1488
- Zeles-Hahn, M.G. *et al.* (2011) Effect of electrostatic spray on human pulmonary epithelial cells. *J. Electrostat.* 69, 67–77
- Fang, X. and Reneker, D.H. (1997) DNA fibers by electrospinning. *J. Macromol. Sci. Phys.* B36, 169–173
- Grabow, W.W. and Jaeger, L. (2014) RNA self-assembly and RNA nanotechnology. *Acc. Chem. Res.* 47, 1871–1880
- Cao, H. *et al.* (2010) RNA interference by nanofiber-based siRNA delivery system. *J. Control. Release* 144, 203–212
- Alyamkina, E.A. *et al.* (2009) Combined therapy with cyclophosphamide and DNA preparation inhibits the tumor growth in mice. *Genet. Vaccines Ther.* 7, 12
- Gulfam, M. *et al.* (2012) Anticancer drug-loaded gliadin nanoparticles induce apoptosis in breast cancer cells. *Langmuir* 28, 8216–8223



- 19 Mottaghtalab, F. *et al.* (2015) Silk fibroin nanoparticle as a novel drug delivery system. *J. Control. Release* 206, 161–176
- 20 Qu, J. *et al.* (2014) Silk fibroin nanoparticles prepared by electrospray as controlled release carriers of cisplatin. *Mat. Sci. Eng. C. Mater. Biol. Appl.* 44, 166–174
- 21 Nyström, M. *et al.* (2015) Solid state transformations in consequence of electrospraying—a novel polymorphic form of piroxicam. *Eur. J. Pharm. Biopharm.* 89, 182–189
- 22 Khan, H. *et al.* (2014) Smart microneedle coatings for controlled delivery and biomedical analysis. *J. Drug. Target* 22, 790–795
- 23 Loscertales, I.G. *et al.* (2002) Micro/nano encapsulation via electrified coaxial liquid jets. *Science* 295, 1695–1698
- 24 Labbaf, S. *et al.* (2014) Preparation of multilayered polymeric structures using a novel four-needle coaxial electrohydrodynamic device. *Macromol. Rapid. Commun.* 35, 618–623
- 25 Rasekh, M. *et al.* (2015) Hollow-layered nanoparticles for therapeutic delivery of peptide prepared using electrospraying. *J. Mater. Sci. Mater. Med.* 26, 256
- 26 Zamani, M. *et al.* (2014) Protein encapsulated core-shell structured particles prepared by coaxial electrospraying: investigation on material and processing variables. *Int. J. Pharm.* 473, 134–143
- 27 Laelorspoen, N. *et al.* (2014) Microencapsulation of *Lactobacillus acidophilus* in zein-alginate core-shell microcapsules via electrospraying. *J. Funct. Foods* 7, 342–349
- 28 Ghayempour, S. and Mortazavi, S.M. (2013) Fabrication of micro-nanocapsules by a new electrospraying method using coaxial jets and examination of effective parameters on their production. *J. Electrostat.* 71, 717–727
- 29 Hao, S. *et al.* (2015) Porous hydrophilic core/hydrophobic shell nanoparticles for particle size and drug release control. *Mater. Sci. Eng. C. Mater. Biol. Appl.* 49, 51–57
- 30 Cao, Y. *et al.* (2014) Dual drug release from core-shell nanoparticles with distinct release profiles. *J. Pharm. Sci.* 103, 3205–3216
- 31 Yan, E. *et al.* (2014) Biocompatible core-shell electrospun nanofibers as potential application for chemotherapy against ovary cancer. *Mater. Sci. Eng. C. Mater. Biol. Appl.* 41, 217–223
- 32 Yang, G. *et al.* (2015) An implantable active-targeting micelle-in-nanofiber device for efficient and safe cancer therapy. *ACS Nano* 9, 1161–1174
- 33 Qian, W. *et al.* (2013) Triple-component drug-loaded nanocomposites prepared using a modified coaxial electrospinning. *J. Nanomater.* 2013, 826471
- 34 Huang, W. *et al.* (2013) Drug-loaded zein nanofibers prepared using a modified coaxial electrospinning process. *AAPS PharmSciTech* 14, 675–681
- 35 Raheja, A. *et al.* (2013) Studies on encapsulation of bovine serum albumin, lysozyme and insulin through coaxial electrospinning. *J. Biomater. Tissue Eng.* 3, 669–672
- 36 Ranjbar-Mohammadi, M. *et al.* (2016) Gum tragacanth/poly(L-lactic acid) nanofibrous scaffolds for application in regeneration of peripheral nerve damage. *Carbohydr. Polym.* 140, 104–112
- 37 Gao, Y. *et al.* (2016) Optimising the shell thickness-to-radius ratio for the fabrication of oil-encapsulated polymeric microspheres. *Chem. Eng. J.* 284, 963–971
- 38 Wang, B. *et al.* (2016) Hollow polycaprolactone composite fibers for controlled magnetic responsive antifungal drug release. *Colloids Surf. B.* 145, 757–767
- 39 Hayashi, K. *et al.* (2010) Electrosprayed synthesis of red-blood-cell-like particles with dual modality for magnetic resonance and fluorescence imaging. *Small* 6, 2384–2391
- 40 Regele, J.D. *et al.* (2002) Effects of capillary spacing on EHD spraying from an array of cone jets. *J. Aerosol Sci.* 33, 1471–1479
- 41 Yang, Y. *et al.* (2010) A shield ring enhanced equilateral hexagon distributed multi-needle electrospinning spinneret. *IEEE Trans. Dielectr. Electr. Insul.* 17, 1592–1601
- 42 Liu, W. *et al.* (2013) Preparation of multilayer biodegradable nanofibers by triaxial electrospinning. *ACS Macro Lett.* 2, 466–468
- 43 Han, D. and Steckl, A.J. (2013) Triaxial electrospun nanofiber membranes for controlled dual release of functional molecules. *ACS Appl. Mater. Interf.* 5, 8241–8245
- 44 Yarin, A.L. and Zussman, E. (2004) Upward needleless electrospinning of multiple nanofibers. *Polymer* 45, 2977–2980
- 45 Bocanegra, R. *et al.* (2005) Multiple electrosprays emitted from an array of holes. *J. Aerosol Sci.* 36, 1387–1399
- 46 Zhang, C. *et al.* (2015) Stable single device multi-pore electrospaying of polymeric microparticles via controlled electrostatic interactions. *RSC Adv.* 5, 87919–87923
- 47 Mou, F. *et al.* (2013) Oppositely charged twin-head electrospray: a general strategy for building Janus particles with controlled structures. *Nanoscale* 5, 2055–2064
- 48 Rahmani, S. *et al.* (2015) Long-circulating Janus nanoparticles made by electrohydrodynamic co-jetting for systemic drug delivery applications. *J. Drug Target* 23, 750–758
- 49 Li, Y. *et al.* (2008) Microbubble suspensions prepared via electrohydrodynamic jetting process. *Int. Confer. Biomed. Eng. Informat.* 2, 445–449
- 50 Farook, U. *et al.* (2009) Preparation of suspensions of phospholipid-coated microbubbles by coaxial electrohydrodynamic atomization. *J. R. Soc. Interface* 6, 271–277
- 51 Ekemen, Z. *et al.* (2011) Fabrication of biomaterials via controlled protein bubble generation and manipulation. *Biomacromolecules* 12, 4291–4300
- 52 Ekemen, Z. *et al.* (2013) Electrohydrodynamic bubbling: an alternative route to fabricate porous structures of silk fibroin based materials. *Biomacromolecules* 14, 1412–1422
- 53 Mahaingam, S. *et al.* (2014) Formation, stability, and mechanical properties of bovine serum albumin stabilized air bubbles produced using coaxial electrohydrodynamic atomization. *Langmuir* 30, 6694–6703
- 54 Youn, D. *et al.* (2009) Electrohydrodynamic micropatterning of silver ink using near-field electrohydrodynamic jet printing with tilted-outlet nozzle. *Appl. Phys. A. Mater. Sci. Process* 96, 933–938
- 55 Park, J. *et al.* (2007) High-resolution electrohydrodynamic jet printing. *Nat. Mater.* 6, 782–789
- 56 Thian, E.S. *et al.* (2008) The role of electrosprayed apatite nanocrystals in guiding osteoblast behaviour. *Biomaterials* 29, 1833–1843
- 57 Gupta, A. *et al.* (2007) Novel electrohydrodynamic printing of nanocomposite biopolymer scaffolds. *J. Bioact. Compatible Polym.* 22, 265–280
- 58 Rasekh, M. *et al.* (2011) Direct writing of polycaprolactone polymer for potential biomedical engineering applications. *Adv. Eng. Mater.* 13, B296–B305
- 59 Wang, J. *et al.* (2016) Fabrication of patterned polymer-antibiotic composite fibers via electrohydrodynamic (EHD) printing. *J. Drug Deliv. Sci. Tec.* 35, 114–123
- 60 Ahmad, Z. *et al.* (2012) Antimicrobial properties of electrically formed elastomeric polyurethane-copper oxide nanocomposites for medical and dental applications. *Meth. Enzymol.* 509, 87–99
- 61 Kim, Y. *et al.* (2015) High-resolution electrohydrodynamic printing of silver nanoparticle ink via commercial hypodermic needles. *Appl. Phys. Lett.* 106, 014103
- 62 Lee, H. *et al.* (2014) Direct alignment and patterning of silver nanowires by electrohydrodynamic jet printing. *Small* 10, 3918–3922